



Two-dimensional Parameter Relationships for W UMa-type Systems Revisited

Atila Poro¹ , Ehsan Paki¹ , Ailar Alizadehsabegh² , Mehdi Khodadadilori³ , Selda Ranjbar Salehian⁴ ,
Mahya Hedayatjoo⁵ , Fatemeh Hashemi⁶ , Yasaman Dashti⁷ , and Fatemeh Mohammadizadeh⁸ 

¹Astronomy Department of the Raderon AI Lab., Burnaby, BC, Canada; poroatila@gmail.com

²Faculty of Electrical and Computer Engineering, Department of Photonics, University of Tabriz, Tabriz 51664, Iran

³Department of Electrical Engineering, Amirkabir University of Technology, Tehran, Iran

⁴Astronomy Students' Scientific Association, University of Tabriz, Tabriz 51664, Iran

⁵Department of Physics, Iran University of Science and Technology, Tehran, Iran

⁶Institute for the Intellectual Development (Kanoon), Astronomy Group, Bojnord, Iran

⁷Department of Mechanical Engineering, Amirkabir University of Technology, Tehran, Iran

⁸Aerospace Engineering Department, Science and Research Branch of Islamic Azad University, Tehran, Iran

Received 2023 July 22; revised 2023 October 23; accepted 2023 October 30; published 2023 December 12

Abstract

Reviewing the empirical and theoretical parameter relationships between various parameters is a good way to understand more about contact binary systems. In this investigation, two-dimensional (2D) relationships for $P-M_{V(\text{system})}$, $P-L_{1,2}$, $M_{1,2}-L_{1,2}$, and $q-L_{\text{ratio}}$ were revisited. The sample used is related to 118 contact binary systems with an orbital period shorter than 0.6 days whose absolute parameters were estimated based on the Gaia Data Release 3 parallax. We reviewed previous studies on 2D relationships and updated six parameter relationships. Therefore, Markov chain Monte Carlo and Machine Learning methods were used, and the outcomes were compared. We selected 22 contact binary systems from eight previous studies for comparison, which had light curve solutions using spectroscopic data. The results show that the systems are in good agreement with the results of this study.

Key words: (stars:) binaries (including multiple): close – stars: fundamental parameters – methods: data analysis

1. Introduction

The W Ursae Majoris (W UMa) stars are one of the most interesting types of binary systems, and they are important astrophysical tools for understanding star formation, structure, and evolution. Both stars in these contact binary systems have exceeded their Roche lobes, and mass transfer through Lagrange points is likely to occur. The W UMa-type systems are known as Low-Temperature Contact Binaries (LTCBs), and the difference between the temperatures of two components in these types of eclipsing stars is close to equal (Yakut & Eggleton 2005).

W UMa binary systems typically have orbital periods of less than one day, but different intervals are specifically defined for contact binaries (e.g., Qian 2003; Joshi & Jagirdar 2017; Qian et al. 2017; Chen et al. 2018; Kouzuma 2018; Jayasinghe et al. 2020; Latković et al. 2021; Poro et al. 2022a, 2022b). However, according to the Latković et al. (2021) study, systems with an orbital period and temperature of more than 0.5 days and 7000 K respectively are likely to have radiative envelopes and should not be classified as W UMa-type binaries.

Although there have been many theoretical and observational research publications, our knowledge of contact binary stars is still far from complete. The relationships between the absolute parameters in W UMa-type systems continue to be

ambiguous, especially in view of the various techniques for the analysis of light curves and the number of contact binary systems that have been studied. There are some strong and weak trends in the relationships between parameters; however, it appears that these results depend on the sample and the method used to study the relationships. For this reason, investigations of these relationships by using modern methods are always useful.

In this study, we continue to use a sample of absolute parameters for 118 contact systems estimated in the Poro et al. (2022b) study. The aim is to investigate the relationship between some parameters in two-dimensional (2D) space. This paper's structure is as follows: The data used to analyze the relationships between parameters are described in Section 2; the relationships between the orbital period, mass, and luminosity of the contact binary systems are discussed in Sections 3 and 4; updated relations and related methods are presented in Section 5; and finally, there is a conclusion in Section 6.

2. Dataset

The Poro et al. (2022b) investigation employed 118 contact systems with orbital periods less than 0.6 days, and we used

Table 1
Calculated Systems' Absolute Magnitudes of the Sample

System	M_V	System	M_V	System	M_V	System	M_V
ASAS J212234-4627.6	4.506(38)	AB And	5.608(58)	BH Cas	4.200(160)	MU Cnc	4.946(246)
ASAS J212319-4622.4	4.896(169)	GZ And	4.354(67)	V573 Peg	3.664(214)	V596 Peg	5.216(221)
ASAS J174406+2446.8	4.193(33)	AO Cam	4.779(382)	EP And	3.409(317)	V658 Lyr	3.942(58)
1SWASP J064501.21+342154.9	6.626(342)	DK Cyg	2.559(236)	AP Leo	3.428(34)	V700 Cyg	4.920(102)
2MASS 02 272 637+1156494	7.393(172)	KW Psc	6.242(151)	BI CVn	3.668(189)	FZ Ori	3.430(258)
ASAS J083241+2332.4	3.896(52)	LO And	3.805(202)	AL Cas	2.995(52)	LP UMa	4.298(77)
1SWASP J155822.10-025604.8	5.418(27)	V1191 Cyg	4.200(340)	V680 Per	3.399(106)	FP Lyn	3.882(126)
1SWASP J212808.86+151622.0	6.954(29)	V1853 Ori	3.775(193)	EZ Hydrae	3.770(248)	FV CVn	4.584(36)
UCAC4 436-062932	4.842(36)	CE Leo	5.558(22)	MQ UMa	2.513(64)	V354 UMa	4.418(74)
TYC 1597-2327-1	5.359(197)	V532 Mon	3.119(181)	V1197 Her	6.163(50)	OQ Cam	3.220(257)
1SWASP J080150.03+471433.8	6.398(378)	GU Ori	3.547(267)	AH Cnc	3.759(229)	EQ Tau	4.522(263)
J015829.5+260333	3.500(127)	FI Boo	4.034(28)	V781 Tau	3.735(42)	V737 Per	4.622(295)
J030505.1+293443	6.179(195)	AV Pup	3.21(64)	V1848 Ori	5.702(124)	V336 TrA	5.626(95)
SDSS J012119.10-001949.9	7.443(71)	NN Vir	2.229(23)	QQ Boo	4.801(219)	HN Psc	4.158(86)
1SWASP J140533.33+114639.1	6.453(212)	AQ Psc	2.893(80)	V608 Cas	3.961(232)	V685 Peg	4.795(305)
ROTSE1 J164341.65+251748.1	4.581(381)	XY Leo	5.481(29)	QX And	3.005(116)	BO Ari	4.287(30)
GSC 03 526-01995	5.644(374)	V2284 Cyg	4.88(167)	UY UMa	3.539(163)	V351 Peg	1.849(38)
GSC 3581-1856	5.493(166)	GK Aqr	5.100(248)	BF Pav	4.999(137)	AK Her	3.176(24)
GSC 1042-2191	2.760(27)	V396 Mon	4.052(350)	AA UMa	3.489(148)	HI Dra	1.755(22)
NSVS 2 701 634	5.968(152)	TT Cet	2.670(71)	NR Cam	5.385(167)	V1128 Tau	4.556(33)
NSVS 2 643 686	3.398(338)	PS Vir	4.731(35)	V776 Cas	2.258(26)	V2612 Oph	3.789(39)
NSVS 7 245 866	3.374(179)	BQ Ari	5.114(56)	PY Vir	5.287(83)	EP Cep	5.419(195)
NSVS 1 557 555	5.127(50)	V870 Ara	3.546(79)	RZ Tau	3.307(105)	EQ Cep	5.507(170)
GSC 2723-2376	5.080(68)	V811 Cep	5.550(121)	EH CVn	5.829(62)	ES Cep	4.107(153)
GSC 4946-0765	5.276(43)	V842 Cep	4.674(311)	EF CVn	4.858(119)	V369 Cep	4.922(184)
V2240 Cyg	2.734(82)	TZ Boo	4.239(171)	V584 Cam	3.497(121)	V370 Cep	4.635(160)
V1370 Tau	4.568(177)	GW Boo	2.502(122)	GR Vir	3.929(22)	V782 Cep	4.342(74)
V1007 Cas	4.631(190)	BE Cep	4.014(218)	FG Hydrae	4.130(104)	GW Cnc	5.105(245)
V789 Her	4.677(250)	VZ Psc	6.413(339)	UX Eri	3.834(172)	DF CVn	4.820(256)
NX Cam	2.141(96)	RT LMi	3.614(269)				

this sample and results in our study. These systems vary from apparent magnitudes 7 to 17 in the V filter, and they are all A or W type contact binaries from both hemispheres. Considering that both subtypes of W UMa are used in the sample, identifying which star is primary and which one is secondary is based on the study that is used as the reference study for each system. Reference papers include both types of photometric and spectroscopic studies.

In the Poro et al. (2022b) study, the orbital period and the parameters obtained from the light curve solutions are taken from the literature, and absolute parameters for them are determined using the Gaia Data Release 3 (DR3) parallax. The parameters $d(\text{pc})$, A_V , $V_{\text{max}}(\text{mag})$, $l_{1,2}/l_{\text{tot}}$, $BC_{1,2}$, $T_{1,2}$, $r_{\text{mean}1,2}$, and $P(\text{day})$ are needed for estimation of absolute parameters. $M_{V(\text{system})}$, $M_{V1,2}$, $M_{\text{bol}1,2}$, $L_{1,2}$, $R_{1,2}$, $a_{1,2}$, and $M_{1,2}$ are calculated, respectively.

It is remarkable that Poro et al. (2022b) mentioned current research on the systematic zero-point offset of the Gaia DR3 parallaxes and their values that need to be adjusted.

Based on the Poro et al. (2022b) study, the obtained total mass compared to the total mass from the literature that used

the photometric method shows about an 18 percent improvement over spectroscopic investigations.

We obtained the absolute magnitude parameter of each system since it was required in our analysis. The absolute magnitude of each system is calculated using Equation (1)

$$M_{V(\text{system})} = V - 5 \log(d) + 5 - A_V, \quad (1)$$

where V is the maximum apparent magnitude of the system, $d(\text{pc})$ is the distance of the system calculated by using Gaia DR3⁹ parallax, the extinction coefficient is A_V , and its uncertainty was estimated using the DUST-MAPS PYTHON package of Green et al. (2019). The computation results are outlined in Table 1.

3. Period–Luminosity Relationship

There are interesting features of W UMa-type systems that make them special for study, for instance, the existence of a common envelope to transfer mass and energy, the dependence of the radii ratio on the mass ratio through Kuiper's relation

⁹ <https://gea.esac.esa.int/archive/>

Table 2
Some of the Orbital Period, Mass, and Luminosity Relations Presented by Previous Investigations for Contact Systems

Parameters	Relation	References
$P-M_V$	$M_V = (-12.0 \pm 2.0)\log P + (-1.5 \pm 0.8)$	Rucinski (2006)
$P-M_V(\max)$	$M_V(\max) = (-9.15 \pm 0.12)\log P + (-0.23 \pm 0.05),$ $\sigma_V = 0.30(\log P < -0.25)$	Chen et al. (2016)
$P-M_V(\max)$	$M_V(\max) = (-4.95 \pm 0.13)\log P + (0.85 \pm 0.02),$ $\sigma_V = 0.35(\log P > -0.25)$	Chen et al. (2016)
$P-L_1$	$L_1 = (13.98 \pm 0.75)P - (3.04 \pm 0.27)$	Latković et al. (2021)
$P-L_2$	$L_2 = (3.66 \pm 0.26)P - (0.69 \pm 0.09)$	Latković et al. (2021)
$M_{\text{ratio}}-L_{\text{ratio}}$	$L_2/L_1 = (M_2/M_1)^{0.92}$	Lucy (1968a)
$M_{\text{ratio}}-L_{\text{ratio}}$	$L_2/L_1 = (M_2/M_1)^{0.96}$	Lucy (1968b)
$M_{\text{ratio}}-L_{\text{ratio}}$	$L_2/L_1 = (M_2/M_1)^{0.92}$	Copeland et al. (1970)
$M_{\text{ratio}}-L_{\text{ratio}}$	$L_2/L_1 = (M_2/M_1)^{0.93}$	Habets & Heintze (1981)
$M_{\text{ratio}}-L_{\text{ratio}}$	$L_2/L_1 = (M_2/M_1)^{0.82}$	Rovithis-Livaniou et al. (1992)
$M_{\text{ratio}}-L_{\text{ratio}}$	$L_2/L_1 = (M_2/M_1)^{1.04}$	Rovithis-Livaniou et al. (1992)
$M_{\text{ratio}}-L_{\text{ratio}}$	$L_2/L_1 = (M_2/M_1)^{4.60}$	Csizmadia & Klagyivik (2004)
$M_{\text{ratio}}-L_{\text{ratio}}$	$L_2/L_1 = (M_2/M_1)^{0.74}$	Awadalla & Hanna (2005)
M_1-L_1	$\log L_1 = (2.92 \pm 0.11)\log M_1 + (0.01 \pm 0.02)$	Latković et al. (2021)
M_2-L_2	$\log L_2 = (0.69 \pm 0.09)\log M_2 + (0.13 \pm 0.05)$	Latković et al. (2021)
$P-M_V\text{-Color}$	$M_V = -4.44 \log P + 3.02(B - V)_0 + 0.12$	Rucinski & Duerbeck (1997)
$P-M_V\text{-Color}$	$M_V = -4.43 \log P + 3.63(V - I)_0 - 0.31$	Rucinski (2004)
$P-M_V\text{-Color}$	$M_V(\text{mean}) = -5.20 \log P + 1.19(G - W1)_0 - 0.09$	Chen et al. (2018)

(Kuiper 1941) and sharing the same Roche surface. Apart from this, it is possible to derive an orbital period–luminosity or an orbital period–absolute magnitude (generally all called $P-L$) relationship for each contact system as a consequence of the common envelope. Eggen’s (1967) investigations using $P-L$ relations of contact binaries seemed to be useful as distance indicators, similar to those of the classical standard candles such as Cepheid stars. Rucinski (1994, 2004) and Chen et al. (2016) published the framework for these relations. However, several investigations reported a variety of results for contact binary systems and provided the period–luminosity relations.

Rucinski (1994) proposed an orbital period–luminosity–color relationship using 18 W UMa-type contact binaries, which was improved by the Rucinski & Duerbeck (1997) study by utilizing 40 W UMa-type cases and Hipparcos parallaxes. Rucinski (2006) constructed a $P-L$ relation using 21 nearby late-type contact binaries, although only 11 members of the sample followed it; therefore, the relation has a large uncertainty. Muraveva et al. (2014) and Pawlak (2016) obtained relations using a sample of eclipsing binaries in the Large Magellanic Cloud (LMC) which led to an unclear $P-L$ relation due to not correcting for the dominant period–color relations. In another study by Chen et al. (2016), the first reliable 10% (1σ) accuracy, the $P-L$ relation was presented using 66 contact binaries that confirmed the use of W UMa-type binaries as distance indicators.

Mateo & Rucinski (2017) investigated a $P-L$ relationship using Tycho-Gaia astrometric solution (TGAS) parallaxes.

They found a steep linear relationship between the absolute magnitude and the orbital period in the orbital period range of 0.22–0.88 days. In order to improve upon the previous studies, Chen et al. (2018) relied on 183 nearby W UMa-type contact binaries with accurate TGAS parallaxes for present $P-L$ relations. In the Chen et al. (2018) study, photometric observations in the G band and mid-infrared bands were also taken into consideration.

In a recent work, Latković et al. (2021) determined the dependence of the absolute parameters on the orbital period and mass ratio. In addition, relations that indicate the dependence are presented. Latković et al. (2021) relied on a sample of 210 W UMa-type systems with orbital periods <0.5 days and $L_1 < 5L_\odot$ for an investigation of luminosity against orbital period. A linear fit through data has determined the $P-L$ relations between the primary and secondary component stars. Table 2 lists some of the relationships found by various investigators.

4. Mass–Luminosity Relationship

W UMa stars are contact binaries with a common convective envelope (CCE) in which the photosphere stands between the inner and outer Lagrangian zero-velocity surfaces (Lucy 1968a, 1968b). The primary star in contact binary systems transfers its mass and luminosity to the secondary one throughout the common envelope between the stars. The light curve shape and the character of the mass ratio–luminosity ratio relation of W UMa-type stars are explained by assuming the

first accepted contact model by Lucy (1968a) and Lucy (1968b). In the mentioned model the luminosity transfers from the more massive star to the less massive one while the two stars are in thermal and geometrical equality. The model explains that both stars touch each other in spite of filling their Roche lobe. Mochnacki (1981) assumed that the energy transfer rate is solely determined by the mass ratio, whereas Kalimeris & Rovithis-Livaniou (2001) proposed that the energy transfer rate in W UMa-type systems is determined by the luminosity of the secondary star. The following assumptions by Kähler (2002a) and Kähler (2002b) show that the rate of the transferred luminosity is variable in time.

Further investigation by Csizmadia & Klagyivik (2004) demonstrated that this transfer parameter is a function of both mass and luminosity ratios. They also affirmed that different types of contact binaries are located in distinct areas on the mass ratio-luminosity ratio diagram. In addition, they found that with respect to energy transfer, systems with mass ratios higher than $q = 0.72$ form an individual group on the diagram which is introduced as the H-subtype contact binary. Furthermore, a model of W UMa binaries was suggested by Stepień (2009) in which the exchanged energy in the components is attained through large-scale circulation in the equatorial plane. This is found to be in agreement with the recent observational results of Rucinski (2015) and Rucinski (2020) on the structural and evolutionary theories of contact binaries. On the other hand, these theories try to explain the very small differences in the effective temperatures of the components of W UMa binary systems. Zhang et al. (2020) also tried to explain the W UMa phenomenon in terms of stellar evolution in contact systems.

A mass-luminary relationship in contact binaries has been considered the most substantial characteristic behavior of W UMa-type stars due to the fact that it leads to an understanding of stellar structure and evolution in these systems. The relation was defined simply as $L \propto M^a$ in which L represents the luminosity ratio and M is the mass ratio. Osaki (1965) showed that the mass ratio and the luminosity ratio in those systems should be equal ($L_2/L_1 = M_2/M_1$) with $a = 1$. Lucy (1968a) found that the relation between the observable luminosity ratio and the ratio of the stellar surfaces is $L_2/L_1 = (M_2/M_1)^{0.92}$. According to the literature, this relation has been improved by several studies (Table 2).

5. Updated Relations and Methods

We employed both Machine Learning (ML) and Markov chain Monte Carlo (MCMC) methods to obtain the best fit and compare the results.

(a) This study used the ML regression approach to find the best polynomial fit for each parameter set. Polynomial regression is a form of regression analysis (Shaeri et al. 2022). The relationship between the independent variable x and

the dependent variable y is not linear but is the polynomial of the n th degree in x (Pedregosa et al. 2011). The equation for polynomial regression is also derived from the linear regression equation (polynomial regression of degree 1), which is defined as

$$y = b_0 + b_1x + b_2x^2 + \dots + b_nx^n + e, \quad (2)$$

where y is the predicted/target output, $b_0 + b_1, \dots, b_n$ are the regression coefficients and x is an independent input variable. We can say that if data are not distributed linearly but instead represent the n th degree of a polynomial, then we use polynomial regression to get the desired output.

A polynomial regression model consists of successive power terms, and degree is the most important parameter in polynomial regression. We use the bootstrap technique to find the best degree parameter for each relation. The bootstrap is a versatile technique that relies on data-driven simulations to make statistical inferences. When combined with robust estimators the bootstrap can afford much more powerful and flexible inferences than what is possible with standard approaches such as t-tests on means. We calculated the Root Mean Square Error (RMSE) for each order and identified the best fit to find the best order for the fractional model. One thousand rounds are used for each relation with 30% of the data as a testing set. The minimum average of the RMSE of all 1000 running rounds in each degree parameter was used as a basis to select the best degree parameter for the polynomial regression of each relation. RMSE can be expressed as

$$\text{RMSE} = \sqrt{\frac{\sum_{i=1}^n (\hat{y}_i - y_i)^2}{n}}, \quad (3)$$

where n is the number of data points, y_i is the i th measurement and \hat{y}_i is its corresponding prediction. Best-fit values of the equation parameters are determined from this paper's data set utilizing a polynomial regression and parameter error calculated by Standard Error Mean (SEM). The data set was split by 15% for training and validation. The regression model is implemented in Python and uses Polynomial Features data preprocessing. The linear regression model is available in the Python Scikit-learn library (Pedregosa et al. 2011).

(b) We also implemented the MCMC approach to fit polynomial models to the data (Hogg & Foreman-Mackey 2018). We applied MCMC to estimate the posterior probability function and the distribution of parameters, which depend on the polynomial coefficients and are consistent with the data set. The optimization was done by the Python library SciPy v1.10.0. We sampled the distribution using 50 walkers and ran the MCMC for 20 000 steps using the emcee Python package (Foreman-Mackey et al. 2013). The MCMC uncertainties are derived from the 16th, 50th, and 84th percentiles of the samples in the marginalized distributions.

2D relationships are displayed in Figure 1 between $P-M_V$, $P-L_{1,2}$, $M_{1,2}-L_{1,2}$ and $q-L_{\text{ratio}}$. Figure 2 shows the MCMC

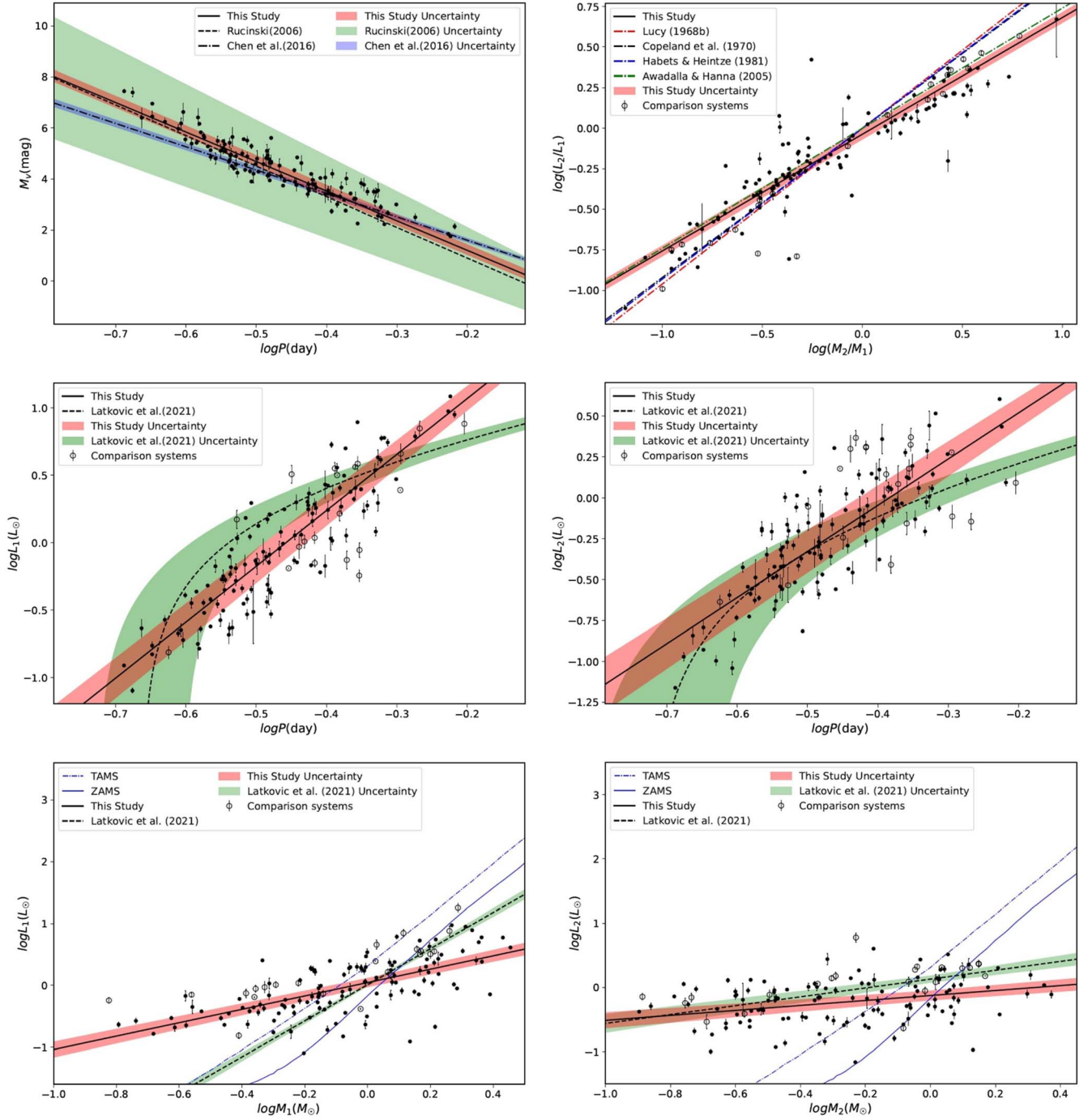


Figure 1. 2D relationships between different parameters in the W UMA-type binary systems. The filled circles correspond to the sample used in this study (118 systems), and the hollow circles are the 22 contact binary systems for comparison. The relations $M_{1,2}-L_{1,2}$ are shown together with the theoretical ZAMS and TAMS.

corner plots of one-dimensional and 2D projections of the posterior probability distributions of polynomial coefficients, and we can see coefficient dependency.

The results of the two MCMC and ML methods were compared, and it was found that the relationships were

precisely the same, with an average difference in uncertainty of only one percent. As a result, we decided to present new relationships using the MCMC approach (Equations (4)–(9)). However, RMSE values for each relationship based on the ML method are as follows: $P-L_1=0.187$, $P-L_2=0.168$,

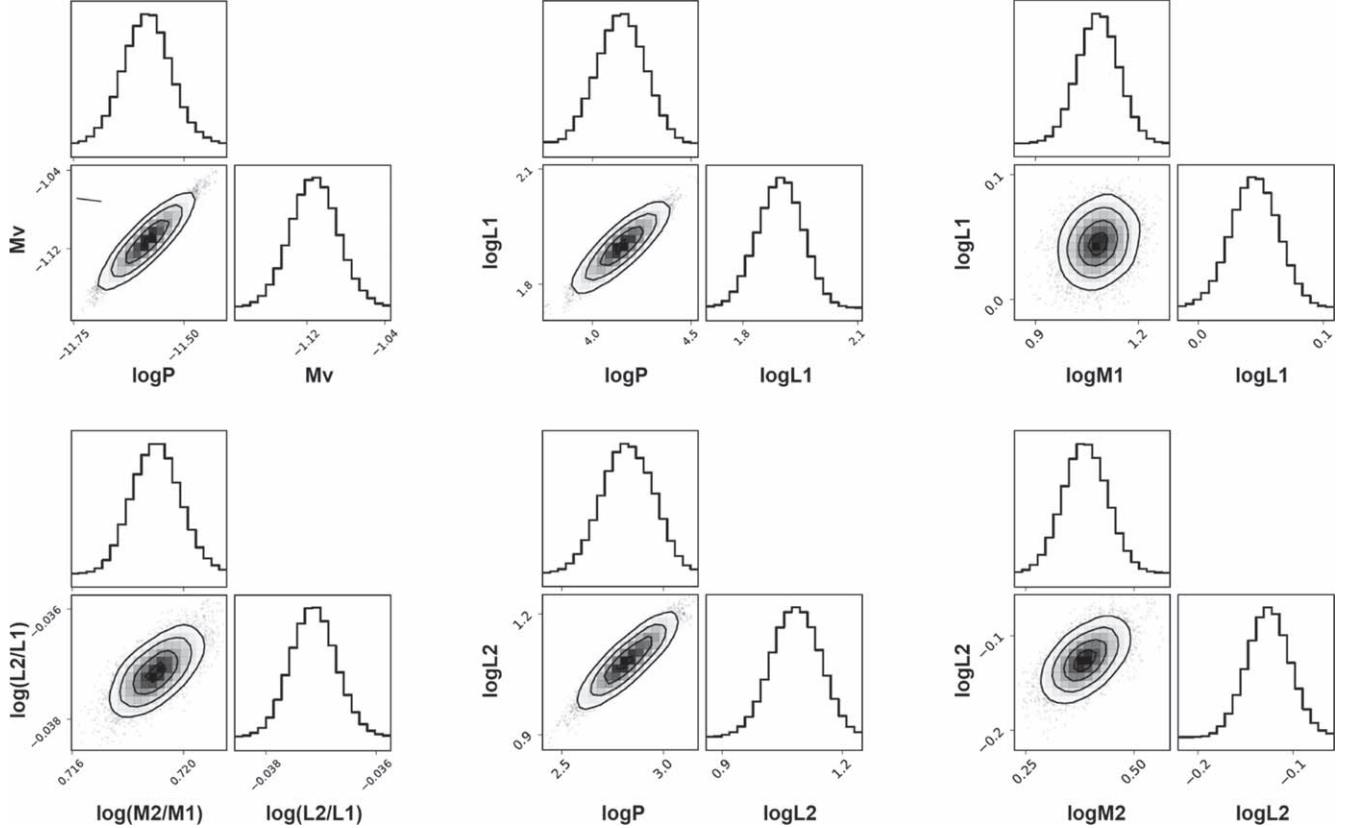


Figure 2. Corner plots of the posterior distribution based on the MCMC sampling.

$M_1-L_1 = 0.323$, $M_2-L_2 = 0.302$, $P-M_{V(\text{system})} = 0.125$ and $q-L_{\text{ratio}} = 0.113$.

Some 2D relations (Table 2) presented by the previous studies are depicted in Figure 1. We display the $P-M_V$ fit related to the Rucinski (2006) study in Figure 1 to illustrate that a significant amount of uncertainty has been taken into account for it.

Moreover, in the relationship of $q-L_{\text{ratio}}$ in Figure 1, we also display four relations from previous studies for comparison. The relationship between $q-L_{\text{ratio}}$ obtained from this study can also be used as $\cong(L_2/L_1) = (M_2/M_1)^{0.72}$ to be comparable with other relationships in Table 2.

In Figure 1, five 2D relationships also affirmed the results of the Latković et al. (2021) study. According to the objectives of the Latković et al. (2021) study, the more massive star is set as star 1, which is different from our sample. Anyway, the logarithmic scale of the relationship of L_1-M_1 presented in the Latković et al. (2021) study reveals that there is a considerable difference compared to this study. However, the 22 comparison contact systems (Figure 1) for L_1-M_1 provide a better agreement with the fit of our investigation. Generally, the samples showed more scatter in the two relations L_1-M_1 and L_2-M_2 than in other relationships.

It should be noted that the two relationships $P-L_{1,2}$ in the Latković et al. (2021) study were not presented on a logarithmic scale. These two relationships do not show a linear fit when converted to logarithmic form. According to Latković et al. (2021) study's sample, the logarithmic scale could be a more appropriate choice for the orbital period interval that they considered.

$$M_V = (-11.58 \pm 0.05) \times \log P + (-1.11 \pm 0.66). \quad (4)$$

$$\log L_1 = (4.15 \pm 0.11) \times \log P + (1.90 \pm 0.13). \quad (5)$$

$$\log L_2 = (2.82 \pm 0.12) \times \log P + (1.08 \pm 0.15). \quad (6)$$

$$\log L_1 = (1.08 \pm 0.06) \times \log M_1 + (0.05 \pm 0.04). \quad (7)$$

$$\log L_2 = (0.39 \pm 0.05) \times \log M_2 + (-0.13 \pm 0.06). \quad (8)$$

$$\log \frac{L_2}{L_1} = (0.72 \pm 0.01) \times \log \frac{M_2}{M_1} + (-0.04 \pm 0.02). \quad (9)$$

6. Discussion and Conclusion

1. Investigating the relationships between different parameters can be helpful for improving our understanding of W UMa-type systems. As is clear in Table 2, in previous studies, investigations have been done with different samples and methods and attempts

Table 3
Selected 22 Contact Binary Systems were Analyzed with Spectroscopic Data to Evaluate Parameter Relationships

System	Type	$P(\text{day})$	$q = M_2/M_1$	$M_1(M_\odot)$	$M_2(M_\odot)$	$L_1(L_\odot)$	$L_2(L_\odot)$	Reference
QX And	A	0.412172	0.306(9)	1.470(50)	0.450(20)	3.160	1.140	Djurašević et al. (2011)
RW Com	W	0.237346	2.123(6)	0.389(20)	0.826(54)	0.154(17)	0.231(23)	Deb & Singh (2011)
OU Ser	A	0.296768	0.173(17)	1.187(99)	0.205(20)	1.488(245)	0.292(81)	Deb & Singh (2011)
V2357 Oph	A	0.415568	0.231(10)	1.160(61)	0.268(25)	1.646(220)	0.390(51)	Deb & Singh (2011)
CK Boo	A	0.355152	0.111(52)	1.584(34)	0.176(8)	3.211(518)	0.572(101)	Deb & Singh (2011)
XX Sex	A	0.540108	0.100(2)	1.301(22)	0.130(6)	7.021(909)	0.717(88)	Deb & Singh (2011)
TW Cet	W	0.316851	1.334(30)	0.722(53)	0.963(97)	0.733(97)	0.886(115)	Deb & Singh (2011)
V2377 Oph	W	0.425406	2.532(12)	0.410(71)	1.038(192)	0.744(120)	1.212(355)	Deb & Singh (2011)
BV Eri	A	0.507655	0.300(20)	1.068(123)	0.320(57)	4.561(822)	0.770(135)	Deb & Singh (2011)
VY Sex	W	0.443433	3.195(5)	0.440(19)	1.406(80)	0.882(119)	2.345(308)	Deb & Singh (2011)
LS Del	W	0.363842	2.666(10)	0.470(138)	1.253(401)	0.933(206)	1.992(403)	Deb & Singh (2011)
V417 Aql	W	0.370314	2.765(7)	0.510(31)	1.410(113)	1.020(117)	2.327(260)	Deb & Singh (2011)
TX Cnc	W	0.382883	2.196(11)	0.602(20)	1.322(57)	1.088(112)	2.030(189)	Deb & Singh (2011)
SZ Hor	A	0.625102	0.470(40)	1.823(159)	0.857(147)	7.605(1.419)	1.234(203)	Deb & Singh (2011)
V839 Oph	W	0.409008	0.305(24)	1.630(24)	0.497(16)	3.550(350)	1.392(138)	Deb & Singh (2011)
DY Cet	A	0.440790	0.356(9)	1.436(34)	0.511(25)	3.840(482)	1.507(194)	Deb & Singh (2011)
V535 Ara	A	0.629306	0.302(3)	1.940(40)	0.590(20)	18(3)	6(1)	Özkardeş & Erdem (2012)
V546 And	W	0.383020	3.937(11)	0.275(8)	1.083(30)	0.706(45)	2.052(41)	Gürol et al. (2015)
KIC 10618253	A	0.437403	0.125(1)	1.476(22)	0.184(3)	3.639(63)	0.698(116)	Şenavcı et al. (2016)
OO Aql	A	0.506792	0.846	1.060(7)	0.897(6)	2.453(7)	1.894(6)	Li et al. (2016)
V972 Her	W	0.443094	6.099(88)	0.150(10)	0.910(70)	0.570(60)	2.110(190)	Selam et al. (2018)
NSVS 4161544	W	0.351680	3.377(5)	0.436(4)	1.473(7)	0.646(4)	1.506(9)	Kjurkchieva et al. (2019)

have been made to reveal the relationships between parameters. This study revisits the relationships between some parameters in 2D space related to contact binary stars using modern methods.

2. A sample of 118 contact binary systems from the Poro et al. (2022b) study was selected. The selection of a sample is important for updating empirical and theoretical relationships. In our sample, the Gaia DR3 parallax method was used to estimate the absolute parameters from the light curve solutions of the selected studies. It should be noted that in the Gaia DR3 parallax method for contact systems if some parameters from the light curve solution have a problem, the values of $a_1(R_\odot)$ and $a_2(R_\odot)$ will not be close to each other and they cannot be averaged to obtain $a(R_\odot)$.

There are some other samples that have been used in previous investigations on contact binary systems' parameter relationships. These samples were gathered to be utilized in those studies, and some changes have been made, such as normalizing the mass ratio and considering more massive stars as primary, which cannot be compared with the current investigation. Some systems in these samples have written the wrong values compared to their study. However, the most important issue to consider is the lack of uniformity in the methods used to estimate absolute parameters in different studies that are considered for samples.

3. We focused on the period–luminosity and mass–luminosity relationships. First, the results of previous studies were reviewed, and then according to our sample and methods, the best fits were determined. MCMC and ML methods were

used for this purpose, and comparing their results showed that they were the same. Consequently, updated parameter relationships were presented for $P-M_{V(\text{system})}$, $P-L_{1,2}$, $M_{1,2}-L_{1,2}$ and $q-L_{\text{ratio}}$ (Equations (4)–(9)). Figure 1 suggests that among these six 2D relationships, $P-L_{1,2}$, $P-M_{V(\text{system})}$, and $q-L_{\text{ratio}}$ have stronger relationships whereas $M_{1,2}-L_{1,2}$ has the weakest.

4. We used a logarithmic scale for the six relationships. Logarithmic scales allow for greater flexibility in analyzing the relationship between parameters. According to performing and comparing relationships with two methods of ML and MCMC in this study, a logarithmic scale increases accuracy. Shorter intervals in the logarithmic scale provide the possibility of a larger number of searches for these two methods, and the best fit could be obtained. Although at first we also checked all relationships with non-logarithmic scales, some relationships in this case required polynomial relationships, but with a logarithmic scale, there was a possibility of a linear fit.

5. Based on the estimation of absolute parameters, $M-L$ is one of the diagrams that shows the evolutionary stage of each star in a contact binary system. The primary star will be near the zero-age main sequence (ZAMS) considering the components in W UMa-type eclipsing binaries share a CCE (Yakut & Eggleton 2005). Usually, primary stars should be more around ZAMS, and we have seen secondary stars near terminal-age main sequence (TAMS) and above it (Figure 1). According to the Yildiz & Doğan (2013) study, the trend is completely opposite for these two stars in W-type systems, which explains

why some stars can be located in unexpected locations in $M_{1,2}$ – $L_{1,2}$ diagrams (Figure 1).

6. We selected 22 different W UMa-type systems than our sample with periods shorter than 0.6 days from eight studies for comparison (Table 3). These systems have analysis with spectroscopic data and also from both A and W types. The stars of the considered systems are in good agreement with the fits and our sample data points, as affirmed in Figure 1. Considering that the absolute magnitude parameter of the systems is not estimated in the studies, it was not possible to display and compare it with the P – $M_{V(\text{system})}$ relationship of this study.

Acknowledgments

The Binary Systems of South and North (BSN) project (<https://bsnp.info/>) and Raderon AI Lab’s Astronomy Department provided scientific support for this study (<https://astronomy.raderonlab.ca/>). We have made use of data from the European Space Agency (ESA) mission Gaia (<http://www.cosmos.esa.int/gaia>), processed by the Gaia Data Processing and Analysis Consortium (DPAC). We would like to thank Golnaz Mazhari, Edwin Budding and Paul D. Maley for their scientific assistance.

ORCID iDs

Atila Poro  <https://orcid.org/0000-0002-0196-9732>
 Ehsan Paki  <https://orcid.org/0000-0001-9746-2284>
 Ailar Alizadehsabegh  <https://orcid.org/0000-0001-5768-0340>
 Mehdi Khodadadilori  <https://orcid.org/0000-0002-9967-6144>
 Selda Ranjbar Salehian  <https://orcid.org/0000-0002-5223-1332>
 Mahya Hedayatjoo  <https://orcid.org/0000-0002-0192-215X>
 Fatemeh Hashemi  <https://orcid.org/0000-0002-0248-1202>
 Yasaman Dashti  <https://orcid.org/0000-0001-8442-6305>
 Fatemeh Mohammadzadeh  <https://orcid.org/0000-0002-9552-6667>

References

Awadalla, N. S., & Hanna, M. A. 2005, *JKAS*, **38**, 43
 Chen, X., de Grijs, R., & Deng, L. 2016, *ApJ*, **832**, 138
 Chen, X., Deng, L., de Grijs, R., Wang, S., & Feng, Y. 2018, *ApJ*, **859**, 140

Copeland, H., Jensen, J. O., & Jorgensen, H. E. 1970, *A&A*, **5**, 12
 Csizmadia, S., & Klagyivik, P. 2004, *A&A*, **426**, 1001
 Deb, S., & Singh, H. P. 2011, *MNRAS*, **412**, 1787
 Djurašević, G., Yılmaz, M., Baştürk, Ö., et al. 2011, *A&A*, **525**, A66
 Eggen, O. J. 1967, *MmRAS*, **70**, 111
 Foreman-Mackey, D., Hogg, D. W., Lang, D., & Goodman, J. 2013, *PASP*, **125**, 306
 Green, G. M., Schlafly, E., Zucker, C., Speagle, J. S., & Finkbeiner, D. 2019, *ApJ*, **887**, 93
 Gürol, B., Bradstreet, D. H., & Okan, A. 2015, *NewA*, **36**, 100
 Habets, G. M. H. J., & Heintze, J. R. W. 1981, *Ap&SS*, **46**, 193
 Hogg, D. W., & Foreman-Mackey, D. 2018, *ApJS*, **236**, 11
 Jayasinghe, T., Stanek, K. Z., Kochanek, C. S., et al. 2020, *MNRAS*, **493**, 4045
 Joshi, Y. C., & Jagirdar, R. 2017, *RAA*, **17**, 115
 Kähler, H. 2002a, *A&A*, **395**, 899
 Kähler, H. 2002b, *A&A*, **395**, 907
 Kalimeris, A., & Rovithis-Livaniou, H. 2001, *OAP*, **14**, 33
 Kjurkchieva, D., Stateva, I., Popov, V. A., & Marchev, D. 2019, *AJ*, **157**, 73
 Kouzuma, S. 2018, *PASJ*, **70**, 90
 Kuiper, G. P. 1941, *ApJ*, **93**, 133
 Latković, O., Čeki, A., & Lazarević, S. 2021, *ApJS*, **254**, 10
 Li, H.-L., Wei, J.-Y., Yang, Y.-G., & Dai, H.-F. 2016, *RAA*, **16**, 2
 Lucy, L. B. 1968a, *ApJ*, **153**, 877
 Lucy, L. B. 1968b, *ApJ*, **151**, 1123
 Mateo, N. M., & Rucinski, S. M. 2017, *AJ*, **154**, 125
 Mochmacki, S. W. 1981, *ApJ*, **245**, 650
 Muraveva, T., Clementini, G., Maceroni, C., et al. 2014, *MNRAS*, **443**, 432
 Osaki, Y. 1965, *PASJ*, **17**, 97
 Özkardeş, B., & Erdem, A. 2012, *NewA*, **17**, 143
 Pawlak, M. 2016, *MNRAS*, **457**, 4323
 Pedregosa, F., Varoquaux, G., Gramfort, A., et al. 2011, *JMLR*, **12**, 2825
 Poro, A., Paki, E., Blackford, M. G., et al. 2022a, *PASP*, **134**, 064201
 Poro, A., Sarabi, S., Zamanpour, S., et al. 2022b, *MNRAS*, **510**, 5315
 Qian, S. 2003, *MNRAS*, **342**, 1260
 Qian, S.-B., He, J.-J., Zhang, J., et al. 2017, *RAA*, **17**, 087
 Rovithis-Livaniou, H., Rovithis, P., & Bitzaraki, O. 1992, *Ap&SS*, **189**, 237
 Rucinski, S. M. 1994, *PASP*, **106**, 462
 Rucinski, S. M. 2004, *NewAR*, **48**, 703
 Rucinski, S. M. 2006, *MNRAS*, **368**, 1319
 Rucinski, S. M. 2015, *AJ*, **149**, 49
 Rucinski, S. M. 2020, *AJ*, **160**, 104
 Rucinski, S. M., & Duerbeck, H. W. 1997, *PASP*, **109**, 1340
 Selam, S. O., Esmer, E. M., Şenavcı, H. V., et al. 2018, *Ap&SS*, **363**, 34
 Şenavcı, H. V., Doğruel, M. B., Nelson, R. H., Yılmaz, M., & Selam, S. O. 2016, *PASA*, **33**, e043
 Shaeri, M. R., Randriambololona, A. M., & Sarabi, S. 2022, Proceedings of the 8th World Congress on Mechanical, Chemical, and Material Engineering (MCM’22), Prague, Czech Republic–July, Vol. 31
 Stępień, K. 2009, *MNRAS*, **397**, 857
 Yakut, K., & Eggleton, P. P. 2005, *ApJ*, **629**, 1055
 Yildiz, M., & Doğan, T. 2013, *MNRAS*, **430**, 2029
 Zhang, X.-D., Qian, S.-B., & Liao, W.-P. 2020, *MNRAS*, **492**, 4112